nature publishing group

Lung transplant acceptance is facilitated by early events in the graft and is associated with lymphoid neogenesis

W Li[1,5], AC Bribriesco[1,5], RG Nava[1], AA Brescia[1], A Ibricevic[2], JH Spahn[1], SL Brody[2], JH Ritter[4], AE Gelman[1,3], AS Krupnick[1], MJ Miller[2] and D Kreisel[1,3]

Early immune responses are important in shaping long-term outcomes of human lung transplants. To examine the role of early immune responses in lung rejection and acceptance, we developed a method to retransplant mouse lungs. Retransplantation into T-cell-deficient hosts showed that for lungs and hearts alloimmune responses occurring within 72 h of transplantation are reversible. In contrast to hearts, a 72-h period of immunosuppression with costimulation blockade in primary allogeneic recipients suffices to prevent rejection of lungs upon retransplantation into untreated allogeneic hosts. Long-term lung acceptance is associated with induction of bronchus-associated lymphoid tissue, where Foxp3$^+$ cells accumulate and recipient T cells interact with CD11c$^+$ dendritic cells. Acceptance of retransplanted lung allografts is abrogated by treatment of immunosuppressed primary recipients with anti-CD25 antibodies. Thus, events contributing to lung transplant acceptance are established early in the graft and induction of bronchus-associated lymphoid tissue can be associated with an immune quiescent state.

INTRODUCTION

Lung transplantation is an established therapy for many patients suffering from end-stage pulmonary disease. Long-term outcomes continue to lag markedly behind those for all other solid organs. Clinical data strongly suggest that early events following engraftment play a critical role in shaping both short- and long-term outcomes after lung transplantation. A recent study from our institution showed that primary graft dysfunction, which is defined by impaired oxygenation and radiological pulmonary infiltrates within the first 72 h of transplantation, is a major risk factor for late death.[1] Furthermore, even a single episode of acute rejection predisposes to late graft failure.[2] These observations suggest that early therapeutic interventions aimed at both innate and adaptive immune responses to lung grafts are important for the success of lung transplantation.

Both experimental studies in rats and clinical observations have indicated that rejection of lungs occurs more rapidly than other organs.[3,4] Our group has recently demonstrated that, unlike the case for all other grafts tested to date, cell trafficking to secondary lymphoid organs is not necessary for lung rejection.[5,6] Lung grafts provide a suitable environment for the initiation of adaptive alloimmune responses and T cells are primed within lung grafts as early as 30 h after transplantation. Thus, pulmonary transplantation poses unique challenges.

Retransplantation models have been valuable in examining the role of graft-resident or graft-infiltrating cells in shaping the fate of tissue or organ transplants.[7,8] One previous study using pulmonary retransplantation in the rat concluded that inflammatory changes induced by acute rejection do not progress, but are irreversible.[9] To address how early alloimmune events impact both rejection and acceptance of pulmonary grafts, we developed techniques for lung retransplantation in the mouse. We show that early rejection occurring within 72 h of lung transplantation is reversible and, similar to the case for heart transplantation, does not suffice to proceed to graft destruction. However, initial transplantation for 72 h into immunosuppressed hosts protects lungs, but not hearts, from rejection after retransplantation into untreated allogeneic recipients. Furthermore, we describe that lung

[1]Department of Surgery, Washington University in St Louis, St Louis, Missouri, USA. [2]Department of Medicine, Washington University in St Louis, St Louis, Missouri, USA. [3]Department of Pathology and Immunology, Washington University in St Louis, St Louis, Missouri, USA. [4]Department of Laboratory Medicine and Pathology, University of Minnesota, Minneapolis, USA. [5]The first two authors contributed equally to this work. Correspondence: D Kreisel (kreiseld@wudosis.wustl.edu)

Received 8 August 2011; accepted 12 March 2012; published online 2 May 2012. doi:10.1038/mi.2012.30

allograft acceptance is associated with induction of bronchus-associated lymphoid tissue (BALT).

RESULTS

Early alloimmune responses are not sufficient for the rejection of pulmonary or cardiac allografts

To evaluate the importance of the first 72 h after transplantation on the immunological outcome, we set out to develop a mouse model of lung retransplantation (**Figure 1a**). To establish the feasibility of lung retransplantation, we first performed syngeneic lung retransplants. At 3 days following transplantation into a syngeneic B6 hosts, the lung B6 grafts were retransplanted into a second B6 recipient. At both 7 and 30 days after retransplantation, grafts were ventilated (**Figure 1b** and **d**). At 7 days, histological examination revealed moderate sequestration of mononuclear cells in the lung interstitium and some thickening of alveolar septae with no perivascular or peribronchial infiltrates (**Figure 1c**). By 30 days after retransplantation, grafts were free of inflammation and the alveolar architecture was well preserved (**Figure 1e**). We have recently shown that lungs provide a suitable environment for the activation of alloreactive T cells and by 3 days after transplantation lung allografts have histological evidence of rejection.[5] To examine whether such early pulmonary allograft rejection is reversible, we employed a previously utilized strategy of organ retransplantation into the original donor strain.[9–11] We therefore transplanted B6 lungs into CBA mice and 72 h later retransplanted these grafts into B6 mice. After 7 days, these grafts had evidence of perivascular cuffing and severe inflammation (**Figure 2a**). However, analogous retransplantation experiments into congenic B6 CD45.1$^+$ recipients (**Figure 2b**) revealed that virtually all graft-infiltrating T cells were derived from the secondary host (**Figure 2c**). A fraction of both graft-infiltrating CD8$^+$ and CD4$^+$ T cells had the capacity to produce interferon-γ. These results indicate that the inflammatory changes in these grafts were due to cells of the second recipient reacting against "passenger" CBA cells that had infiltrated the B6 graft after the initial transplantation. Therefore, we next used T-cell-deficient nude mice as the secondary hosts for B6 lungs 72 h after their initial transplantation into CBA mice. At 7 days after retransplantation into nude recipients, these B6 grafts had histological evidence of acute rejection with perivascular and peribronchial cuffing (**Figure 3a** and **d**), similar to those previously reported 7 days following transplantation of B6 lungs into CBA recipients.[12] However, 30 days after retransplantation the inflammatory changes had resolved and grafts had no evidence of rejection (**Figure 3b** and **d**). Alternatively, B6 lung grafts that were initially transplanted into CBA hosts for 72 h and then retransplanted into CBA recipients had severe graft rejection 30 days later (**Figure 3c** and **d**). We then performed heart retransplants in analogous strain combinations. B6 hearts were acutely rejected after transplantation into CBA hosts (**Figure 4a** and **d**). B6 cardiac grafts first transplanted into allogeneic CBA mice for 72 h and then retransplanted into T-cell-deficient nude recipients maintained a strong heart beat for at least 30 days and had no evidence of rejection (**Figure 4b** and **d**). B6 hearts that were retransplanted into CBA mice after 72 h of initial engraftment in CBA hosts were acutely rejected (**Figure 4c** and **d**). Thus, our findings demonstrate that T cells, which infiltrate lung or heart allografts within the first 72 h of transplantation, are not sufficient to promote graft destruction.

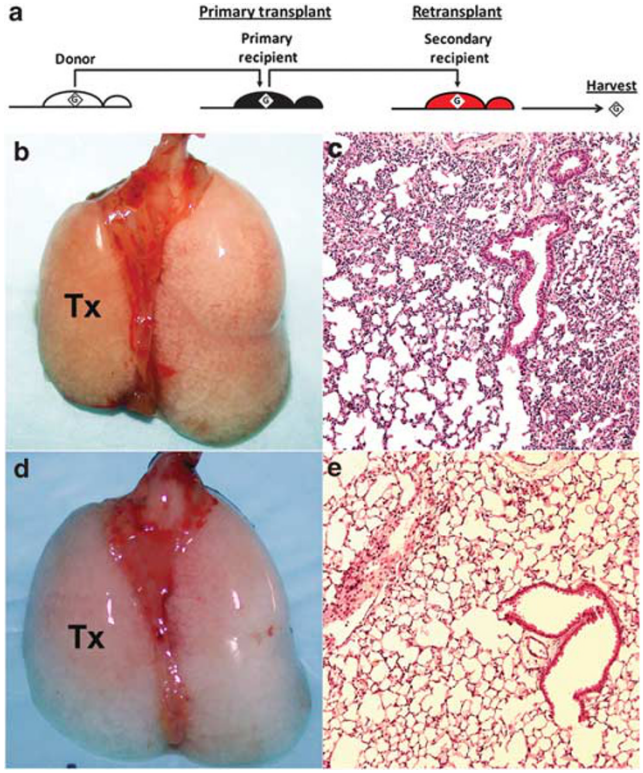

Figure 1 Mouse lung retransplants. (**a**) Schematic outlining retransplantation of organ graft "G" into secondary recipient after initial transplantation into primary host. Gross appearance and histology (hematoxylin and eosin (H&E)) (original magnification, ×100) of B6 lung grafts (Tx), initially transplanted into syngeneic B6 host for 72 h and then retransplanted into B6 mouse shown 7 days (**b**, **c**) (n=4) and 30 days (**d**, **e**) (n=4) after retransplantation.

Early immune responses suffice to protect lung, but not heart allografts from immunological destruction

We have previously reported that perioperative inhibition of the B7-CD28 and CD40-CD40 ligand costimulatory pathways prevents acute rejection and extends graft survival for up to 3 months in a Balb/c→B6 strain combination.[13,14] Similar findings were observed in B6→CBA transplants. B6 grafts are necrotic 30 days after transplantation into nonimmunosuppressed CBA hosts (**Figure 5a** and **e**). By contrast, B6 lungs have only minimal inflammation at this time point, if recipients are treated with MR1 and CTLA4-Ig, and remain ventilated up to 13 months after transplantation (**Figure 5b** and **e** and **Supplementary Figure S1** online). Such grafts develop organized structures around their airways, reminiscent of BALT, which has been previously described in murine and human lungs in the setting of inflammation.[15,16] To examine whether these pulmonary grafts contain cell populations that maintain a tolerant state, we

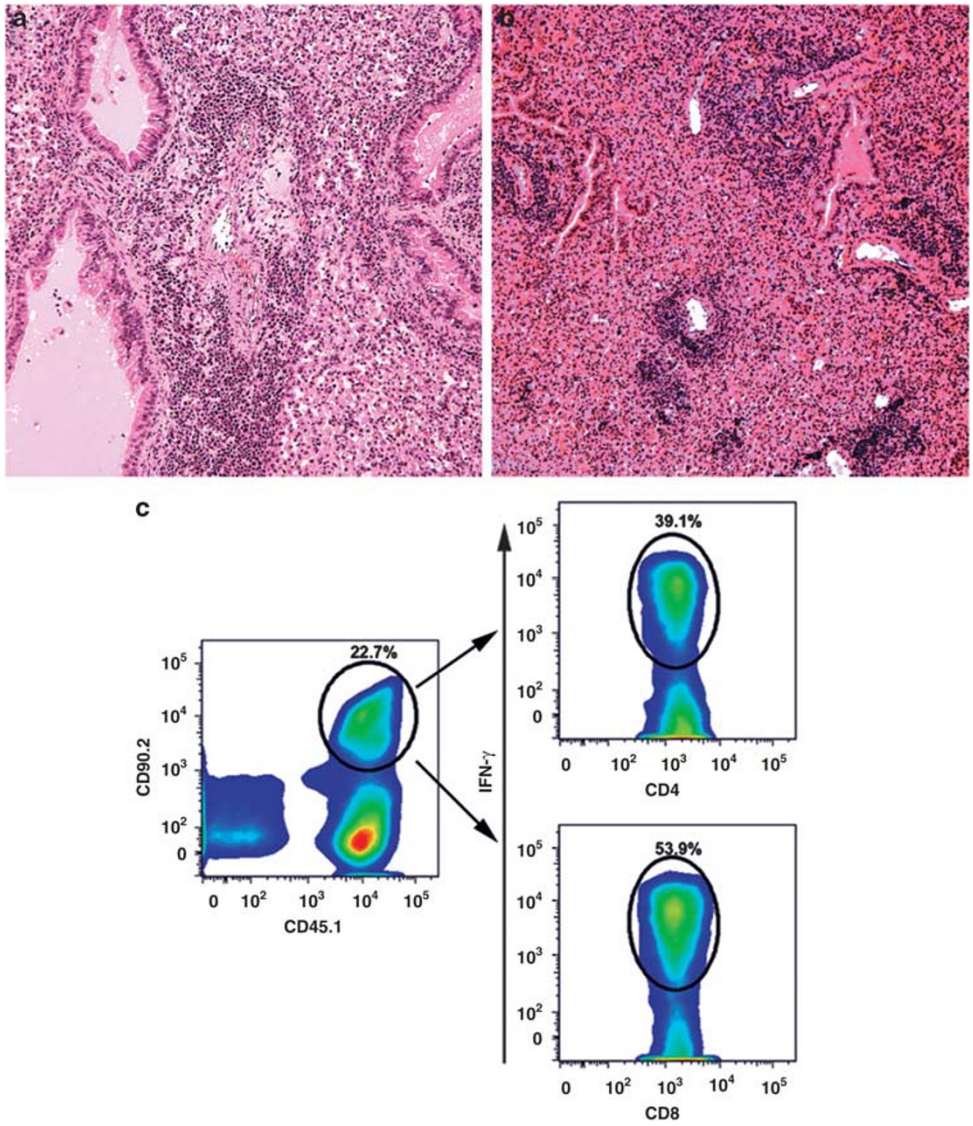

Figure 2 Lung retransplants into wild-type donor strain. Histological appearance (original magnification, ×100) of B6 lung grafts, initially transplanted into CBA recipient for 72 h and then retransplanted into (**a**) B6 or (**b**) B6 CD45.1$^+$ mouse, respectively, shown 7 days after retransplantation. (**c**) Flow cytometric analysis depicting interferon (IFN)-γ production of graft-infiltrating CD4$^+$ and CD8$^+$ T cells for transplants shown in panel **b**. Virtually all graft-infiltrating T cells (CD90.2) are derived from the secondary recipient (CD45.1). Results are representative of at least three transplants in each group.

retransplanted B6 lungs 30 days after initial transplantation into MR1/CTLA4-Ig-treated CBA recipients into secondary nonimmunosuppressed CBA hosts. After 30 days, these retransplanted lungs had minimal inflammation and peribronchial lymphoid aggregates, similar to B6 lungs 30 days after transplantation into immunosuppressed CBA recipients (**Figure 5c** and **e**). Retransplantation of B6 lungs into nonimmunosuppressed CBA recipients 3 days after initial engraftment into immunosuppressed CBA hosts yielded comparable results (**Figure 5d** and **e**). We next set out to examine whether cell populations accumulate within cardiac allografts during 3 days of immunosuppression that can prevent rejection. Similar to lungs, treatment with MR1 and CTLA4-Ig prolonged the survival of B6 cardiac grafts after transplantation into CBA hosts. These grafts maintained a strong heart beat for at least 30 days and had no evidence of rejection (**Figure 6a** and **c**). However, nonimmunosuppressed CBA mice acutely rejected B6 hearts that had been initially maintained in MR1/CTLA4-Ig-treated CBA recipients for 3 days (**Figure 6b** and **c**). The survival of these grafts did not differ from B6 hearts that are transplanted into nonimmunosuppressed CBA hosts (**Figure 4a**). Thus, our results indicate that events occurring within the first 72 h of immunosuppression in lung but not heart transplants suffice to maintain graft survival. Furthermore, such lung acceptance is associated with the formation of lymphoid aggregates within the grafts.

Lung allograft acceptance is associated with induction of BALT

Induction of BALT has been described in various inflammatory pulmonary diseases in mice.[17] Hallmarks of inducible BALT

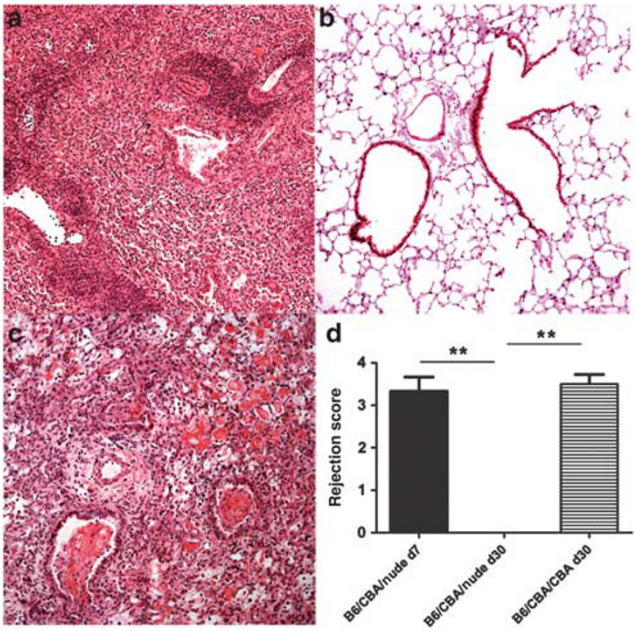

Figure 3 Early alloimmune responses and lung graft rejection. Histological appearance (original magnification, ×100) of B6 lung grafts, initially transplanted into CBA host for 72 h and then retransplanted into nude mouse, shown (**a**) 7 and (**b**) 30 days after retransplantation. (**c**) Histological appearance of B6 lung grafts, initially transplanted into CBA host for 72 h and then retransplanted into secondary CBA recipient shown 30 days (d) after retransplantation. (**d**) Rejection scores (International Society of Heart and Lung Transplantation (ISHLT) grade A) for transplants shown in (**a**) (n=5), (**b**) (n=3), and (**c**) (n=6). (**P<0.01).

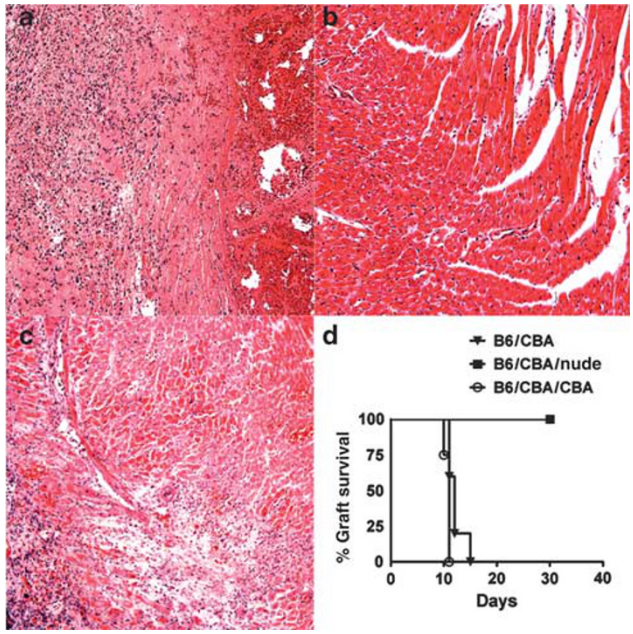

Figure 4 Early alloimmunity and cardiac graft rejection. Histological appearance (original magnification, ×100) of (**a**) B6 hearts transplanted into CBA host (shown at day 12 at the time of cessation of heart beat) (n=4), (**b**) B6 cardiac grafts, initially transplanted into CBA mouse for 72 h and then retransplanted into nude host (killed at 30 days, at which point heart was beating strongly) (n=4), and (**c**) B6 hearts, initially transplanted into CBA mouse for 72 h and then retransplanted into secondary CBA recipient (n=4). (**d**) Graft survival curves for groups shown in (**a**), (**b**), and (**c**), P<0.01 for (**a**) vs. (**b**) and (**c**) vs. (**b**).

include the presence of T cells, B lymphocytes, CD11c$^+$ dendritic cells, and high endothelial venules, as well as expression of homeostatic chemokines. Immunostaining of these structures within accepted primary and retransplanted lung grafts revealed T (CD3$^+$) and B (B220$^+$) lymphocytes (**Figure 7a, b, f,** and **g**). In primary transplants, we occasionally observed separation of B- and T-cell areas (**Figure 7c**), whereas in retransplants T lymphocytes were generally interspersed within B-cell zones (**Figure 7h**). We also detected the expression of peripheral lymph node addressin (PNAd), a hallmark of high endothelial venules (**Figure 7d** and **i**), and CCL21, a ligand for CCR7 (**Figure 7e** and **j**), in both primary transplants and retransplants. We have previously reported that acutely rejected pulmonary allografts do not express features characteristic of BALT.[5] Furthermore, we did not observe organized lymphocytic aggregates in rejected cardiac allografts.

To further assess the morphology of the BALT and the dynamic behavior of T cells in accepted lung grafts, we utilized our recently described technique for intravital two-photon imaging.[18] We transplanted Balb/c lungs into MR1/CTLA4-Ig-treated B6 CD11c-EYFP recipients that express enhanced yellow fluorescent protein under a CD11c promoter,[19] and can therefore be used to identify pulmonary graft-infiltrating CD11c$^+$ dendritic cells.[20] At 30 days after transplantation, we injected CMTMR (4-chloromethyl benzoyl amino tetramethyl rhodamine)-labeled recipient-matched B6T cells into these lung recipients and analyzed the grafts by intravital two-photon imaging 12 h later (**Figure 8**). Unlike the case for pulmonary grafts undergoing acute rejection, where CD11c$^+$ dendritic cells are widely distributed throughout the lung,[20] CD11c$^+$ dendritic cells in accepted lung grafts formed dense cellular aggregates consistent with BALT (**Figure 8a**). Quantitative neighboring analysis revealed that CD11c$^+$ dendritic cells in these regions were significantly more clustered than dendritic cells in other areas of the lung graft (**Figure 8a–c**) and contained a higher density of dendritic cells (**Figure 8d**). Dendritic cells within BALT were often motile and actively probed their local environment with dendrites (**Supplementary Movie 1** online). Moreover, we observed small vessels in dendritic cell aggregates that were distinct in appearance from pulmonary vessels in the remainder of the lung graft or in normal lungs (**Figure 8e** and **f**). Morphologically, these vessels resembled those found in lymph nodes (**Figure 8g**). A quantitative analysis revealed a lower tortuosity index compared with adjacent graft tissue, but a comparable index to vessels in lymph nodes indicating a straighter course (**Figure 8h**). Adoptively transferred T cells interacted extensively with the dendritic cells within these clusters, some making contact with several dendritic cells during the imaging period (**Supplementary Movie 2** online) (**Figure 9a**). Moreover, the majority of T cells within the accepted lung grafts were located within the dendritic

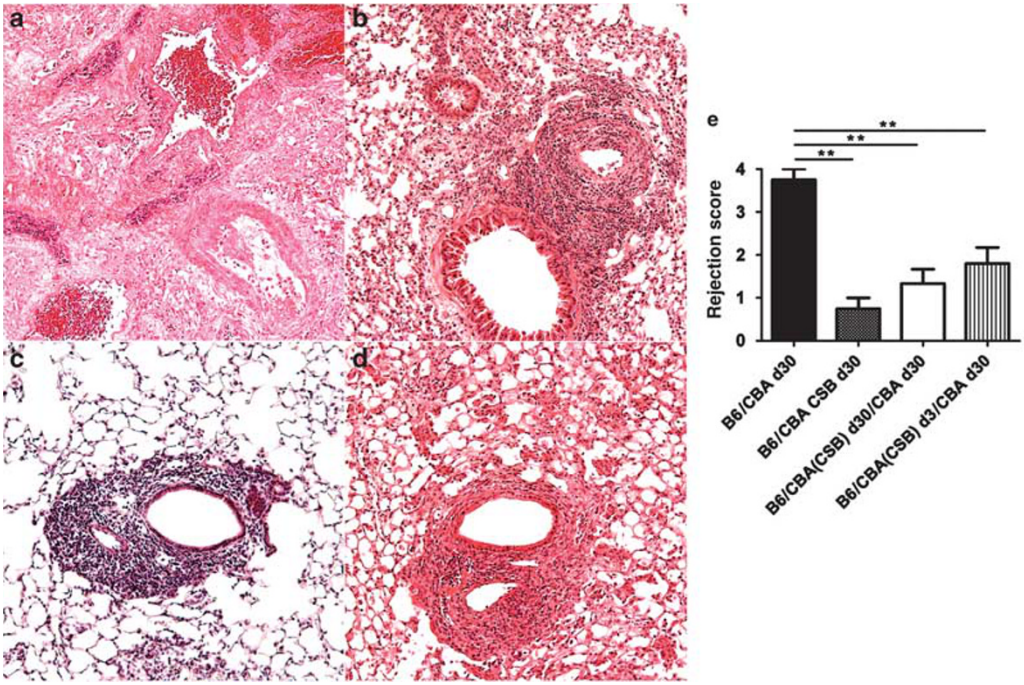

Figure 5 Early responses and lung allograft acceptance. Histological appearance (original magnification, ×100) of B6 grafts 30 days (d) after transplantation into (**a**) untreated ($n=4$) or (**b**) immunosuppressed (MR1 250 μg intraperitoneally (i.p.) day 0, CTLA4-Ig 200 μg i.p. day 2) CBA hosts ($n=6$). Histological appearance of B6 lung grafts, initially transplanted into immunosuppressed CBA hosts for (**c**) 30 days ($n=3$) or (**d**) 72 h ($n=6$) and then retransplanted into untreated CBA mouse shown 30 days after retransplantation. (**e**) Rejection scores (International Society of Heart and Lung Transplantation (ISHLT) grade A) for transplants shown in panels **a**, **b**, **c**, and **d** (**$P<0.01$).

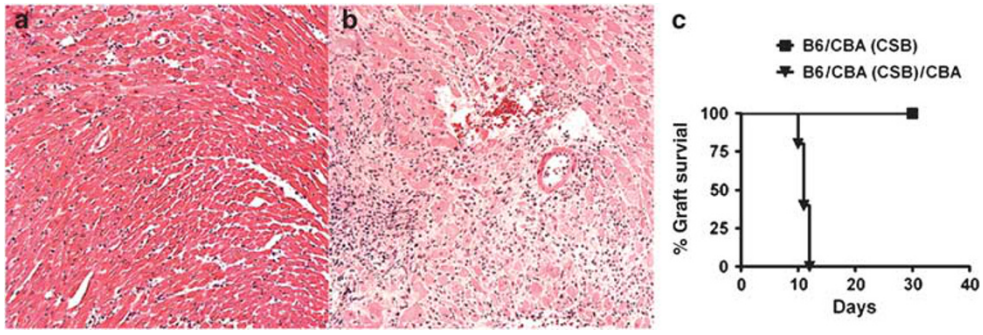

Figure 6 Early responses and cardiac allograft survival. Histological appearance (original magnification, ×100) of (**a**) B6 hearts transplanted into immunosuppressed (MR1 250 μg intraperitoneally (i.p.) day 0, CTLA4-Ig 200 μg i.p. day 2) CBA host (killed at 30 days, at which point heart was beating strongly) ($n=4$) and (**b**) B6 cardiac grafts, initially transplanted into immunosuppressed CBA mouse for 72 h and then retransplanted into untreated CBA host (shown at day 11 at the time of cessation of heart beat) ($n=4$). (**c**) Graft survival curves for groups shown in panels **a** and **b**, $P<0.01$. No statistically significant differences were observed between retransplants depicted here and B6→CBA cardiac transplants shown in **Figure 4** ($P=0.28$).

cell-rich regions (**Figure 9b**), where they displayed low cellular velocities (median track speed 4.08±2.78 μm min^{-1}) (**Figure 9c**), moved randomly with a median meandering index of 0.24±0.25 (**Figure 9d**), and had low displacement (**Figure 9e**). In immunosuppressed Balb→B6 CD11c$^+$ YFP heart transplants that were beating at 30 days, we also observed infiltration of CD11c$^+$ dendritic cells into the cardiac grafts (**Supplementary Figure S2a, b** online). However, in contrast to the lungs, these heart grafts did not have any organized lymphocytic aggregates and did not express PNAd (**Supplementary Figure S2c** online).

Flow cytometric analysis of accepted lung allografts revealed enrichment of T cells that express a regulatory phenotype (CD4$^+$Foxp3$^+$) (**Figure 10a**). The majority of Foxp3-expressing cells were located in the BALT and many were in close proximity to CD11c$^+$ dendritic cells (**Figure 10b**). A portion of CD11c$^+$ dendritic cells within accepted pulmonary allografts expresses the immunoregulatory ligand PD-L1 (**Supplementary Figure S3** online). Treatment of the immunosuppressed CBA lung recipients of B6 lungs with the anti-CD25 monoclonal antibody PC61 prevents graft acceptance upon retransplantation into nonimmunosuppressed CBA hosts (**Figure 10c** and **d**).

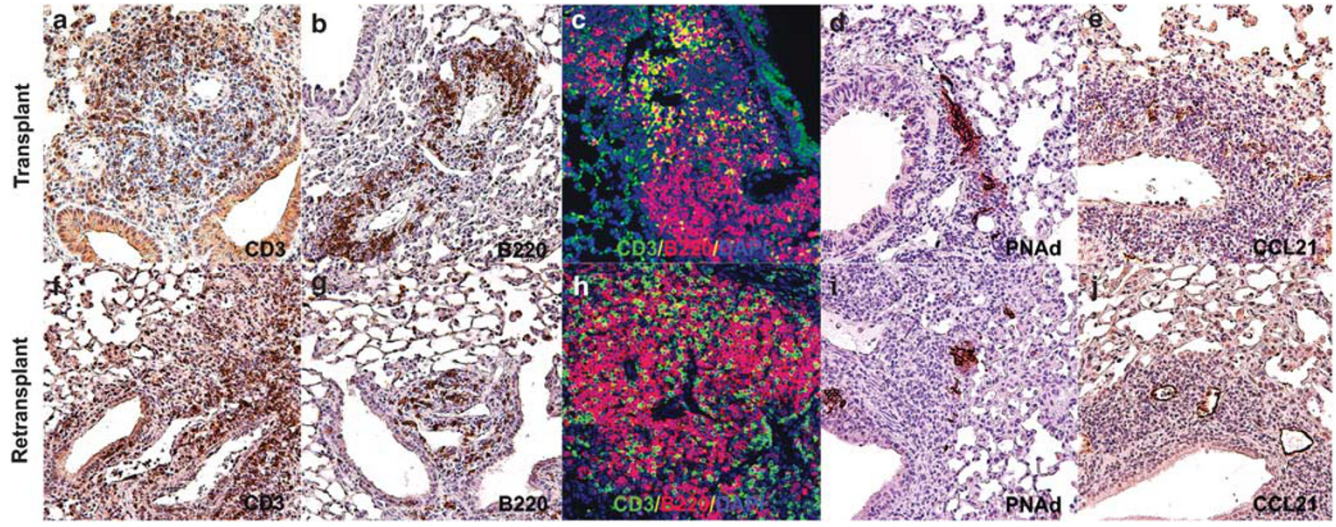

Figure 7 Lymphoid aggregates in accepted lung allografts. Immunostaining (original magnification, ×100) for CD3, B220, peripheral lymph node addressin (PNAd), and CCL21 for B6 grafts 30 days after transplantation into immunosuppressed CBA host (**a**–**e**) or B6 lung grafts, initially transplanted into immunosuppressed CBA host for 72 h and then retransplanted into untreated CBA mouse 30 days after retransplantation (**f**–**j**).

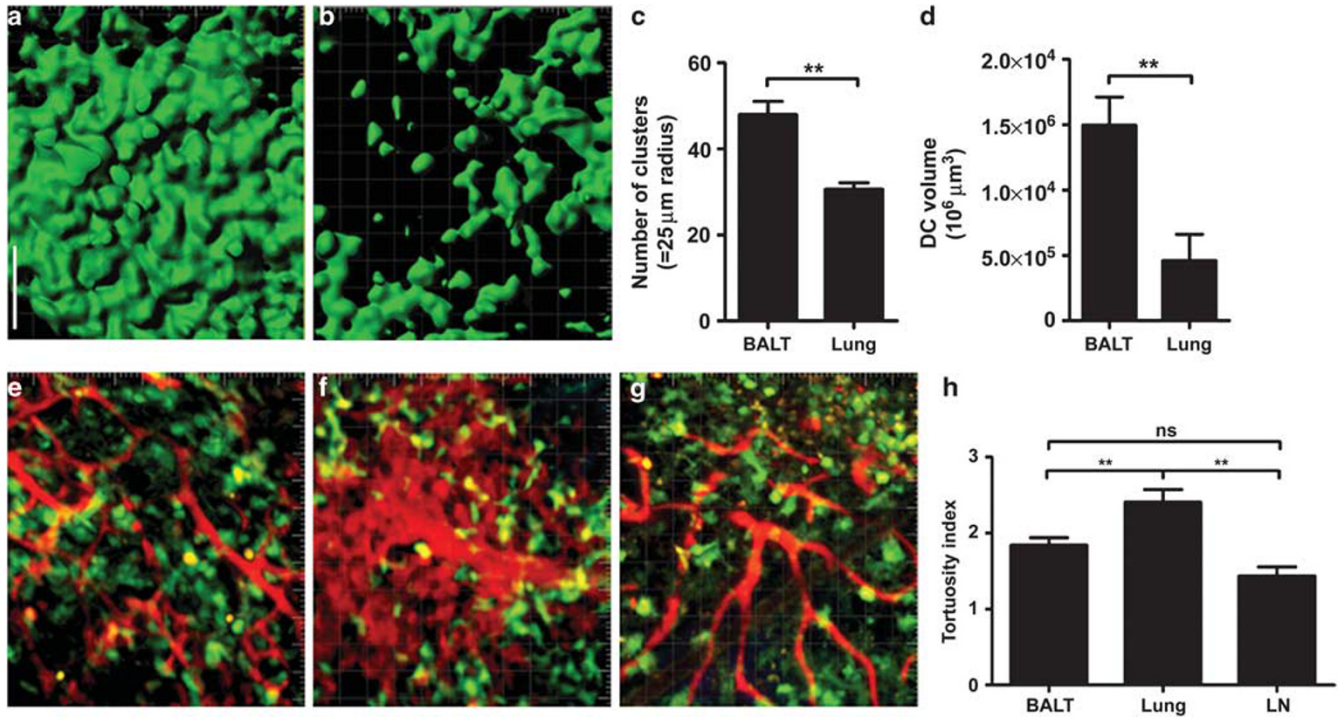

Figure 8 Two-photon images of dendritic cells in accepted Balb/c lung grafts 30 days after transplantation into immunosuppressed (MR1 250 μg intraperitoneally (i.p.) day 0, CTLA4-Ig 200 μg i.p. day 2) B6 CD11c$^+$ EYFP recipients. Dendritic cells (**a**) in bronchus-associated lymphoid tissue (BALT) and (**b**) adjacent graft tissue. (**c**) Neighboring and (**d**) volumetric analysis of dendritic cells within BALT and adjacent lung. Two-photon images of quantum dot (655-nm)-labeled vessels (red) within areas of (**e**) BALT, (**f**) adjacent lung, and (**g**) cervical lymph node. (**h**) Quantitative analysis of tortuosity index of vessels at indicated sites (**$P<0.005$). Bar = 60 μm.

DISCUSSION

Retransplantation of mouse lungs has enabled us to assess the impact of early immune responses on both rejection and acceptance of pulmonary grafts. Our findings extend the notion that immune responses to lungs differ from those to other grafts. We have made several novel observations: (1) early alloimmune responses occurring within the first 72 h after lung transplantation, a time point where we have previously demonstrated marked activation of T cells within pulmonary allografts, are reversible; (2) events occurring in pulmonary, but not

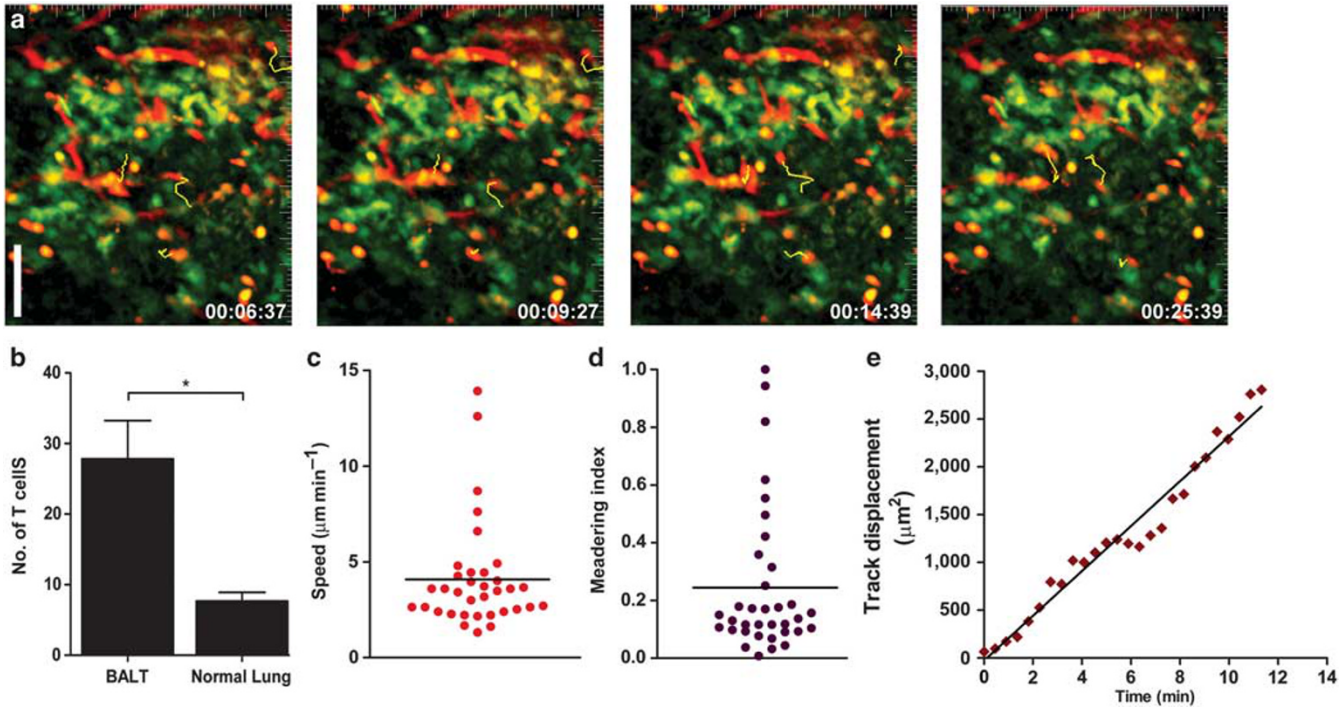

Figure 9 Intravital two-photon imaging of dynamic T-cell behavior within induced bronchus-associated lymphoid tissue (BALT) in accepted Balb/c lung grafts 30 days after transplantation into immunosuppressed (MR1 250 μg intraperitoneally (i.p.) day 0, CTLA4-Ig 200 μg i.p. day 2) B6 CD11c$^+$ EYFP recipients. (**a**) Time-lapse behavior of adoptively transferred 4-chloromethyl benzoyl amino tetramethyl rhodamine (CMTMR)-labeled B6T cells in dendritic cell clusters with tracks indicating representative T cells. Images are individual frames from a continuous time-lapse movie. Relative time is displayed in h:min:s. (**b**) Number of extravasated T cells within BALT and adjacent graft tissue. Plots of (**c**) average track speed (μm min^{-1}) and (**d**) meandering index of extravasated T cells within BALT. Meandering index was calculated by dividing the distance a cell traveled from its starting point by the track length. (**e**) Individual T lymphocytes were tracked and the cell displacement squared (μm^2) vs. time (min) shows a strong linear correlation indicative of random cell migration. $n=35$, $^*P<0.05$, bar = 60 μm.

cardiac allografts within 72 h after transplantation into immunosuppressed recipients protect them from immunological destruction; and (3) lung transplant acceptance is associated with induction of BALT.

We have previously shown that T cells are primed within murine pulmonary grafts within 30 h of transplantation and have undergone multiple rounds of division by 72 h after engraftment.[5] In this study, we demonstrate that these early inflammatory changes are reversible and do not constitute an immunological "point of no return." By contrast, a previous study showed that inflammation persisted for up to 60 days in rat pulmonary grafts that were initially transplanted into allogeneic hosts for 3 or 5 days and subsequently retransplanted into the donor strain.[9] The authors concluded that inflammatory changes in the retransplanted grafts at late time points corresponded to those at the time of retransplantation and were thus not reversible. However, as wild-type donor animals rather than T-cell-deficient recipients were used as secondary hosts, we suggest that the inflammation in the retransplanted grafts may have been due to infiltration of cells that were derived from the secondary recipient.

It is imperative to gain a better understanding of the immunological requirements necessary to achieve lung allograft acceptance. We show that, in contrast to heart transplants, lung allografts that are retransplanted into untreated hosts following an initial 72-h engraftment period into immunosuppressed recipients survive long term. These observations suggest that immunoregulatory pathways are established within lung allografts after only a short period in immunosuppressed hosts. This notion is further supported by the prevention of acceptance of retransplanted lung grafts when the initial immunosuppressed host is treated with an anti-CD25 antibody (PC61) that has been widely used to deplete CD4$^+$Foxp3$^+$ regulatory T cells.[21–23] Previous studies have identified an important role for draining lymph nodes in establishing tolerance following cardiac transplantation.[24] Thus, the failure to achieve long-term survival in heart transplants may be related to a requirement for cell trafficking to secondary lymphoid organs to establish suppression following cardiac, but not lung transplantation.[5,15,25]

Tertiary lymphoid tissue refers to the neoformation of ectopic organized lymphoid aggregates in adult life.[26] Such structures have been observed in many organs and are associated with chronic inflammatory processes. For example, they can be present in livers affected by primary sclerosing cholangitis or in salivary glands of patients suffering from Sjögren's disease.[27,28] The development of tertiary lymphoid organs has been observed in transplanted grafts and has been generally linked to poor outcomes. To this end, tertiary lymphoid tissue has been described

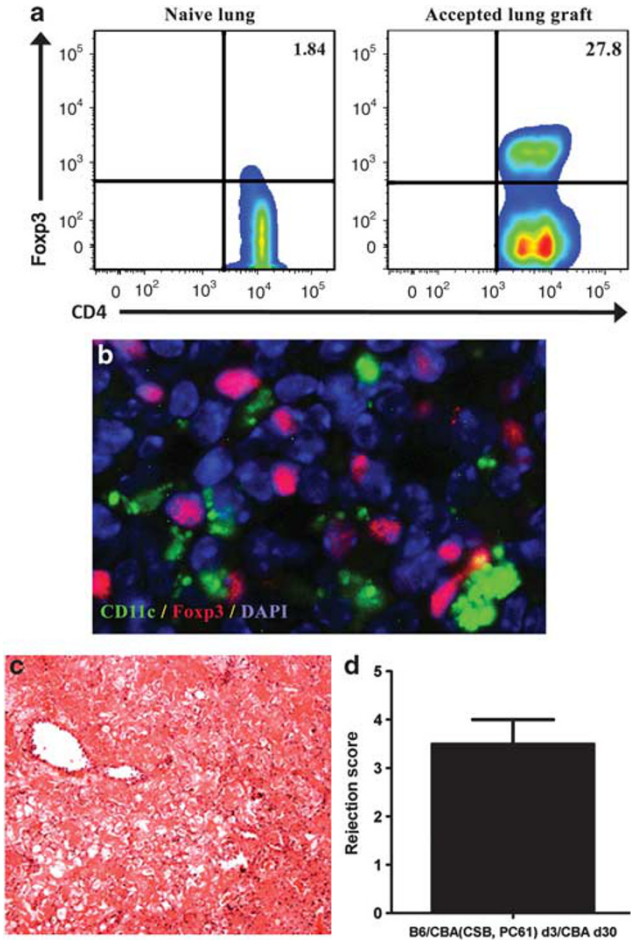

Figure 10 Regulatory T cells in accepted lung grafts. (**a**) Flow cytometric analysis of Foxp3-expressing CD4$^+$ T cells in (left) lungs derived from naive B6 mice (3.01±0.46% (s.e.m.)) and (right) B6 lung allografts 30 days after transplantation into MR1- and CTLA4-Ig-treated CBA mice (21.77±3.55%) (n=3 each). (**b**) Immunofluorescent staining of Foxp3$^+$ cells in bronchus-associated lymphoid tissue (BALT) of Balb/c lung grafts 30 days after transplantation into MR1- and CTLA4-Ig-treated B6 CD11c-EYFP recipient. Foxp3-expressing cells are red, CD11c$^+$ dendritic cells are green, and nucleated cells are blue (4′,6′ diamidino-2-phenylindole (DAPI)). (**c**) Histological appearance and (**d**) rejection score (International Society of Heart and Lung Transplantation (ISHLT) grade A) for B6 lung grafts that were initially transplanted into immunosuppressed (MR1, CTLA4-Ig) CBA recipient that also received PC61 and then retransplanted into nonimmunosuppressed CBA host shown 30 days after retransplantation (n=4).

in chronically rejected human hearts, kidneys, and livers.[29] The small intestine is rich in tertiary lymphoid tissues such as Peyer's patches and cryopatches. Wang *et al.*[30] showed that alloreactive T cells can be primed in donor lymphoid tissue after intestinal transplantation. Although we did not observe organized lymphoid aggregates in acutely rejecting cardiac grafts, Baddoura *et al.*[31] demonstrated an association between lymphoid neogenesis and chronic rejection in mouse heart transplants. On the basis of these observations, the authors suggested that tertiary lymphoid organs could be a site of generation of alloimmune responses that contribute to the development of chronic rejection. Similarly, work by Thaunat *et al.*[29] provided evidence that ectopic lymphoid tissue within chronically rejected grafts plays a role in the generation of local humoral alloimmune responses. Moreover, Nasr *et al.*[32] demonstrated that naïve T cells can be primed within skin graft-resident tertiary lymphoid organs. Thus, targeting lymphoid neogenesis within allografts has been proposed as a potential target to improve outcomes after transplantation. However, the concept that lymphoid neogenesis is necessarily deleterious has been challenged by a recent study, which reported the development of tertiary lymphoid organs within long-term surviving murine kidney allografts.[33]

Tertiary lymphoid tissue in the lung is represented by BALT. In species where BALT is constitutively expressed such as rabbits and rats, it is typically located along major bronchi or at airway bifurcations.[34] In mice and humans, however, where BALT is not expressed at baseline, but can be induced under inflammatory conditions, its location within the lung is more variable.[17] Analogous to our observations in accepted lung allografts, it is often situated next to small pulmonary arteries that are in close proximity to small airways. While BALT can have the appearance of perivascular cuffing, it does not infiltrate the airway epithelium or vascular endothelium.[16,35] BALT can act as a site for the initiation of adaptive immune responses and it has been postulated that chronic inflammation is necessary for its formation.[15] To this end, BALT has been observed in lungs infected with viruses or bacteria, autoimmune diseases, and chronic obstructive pulmonary disease.[15,16,36] Two studies examining BALT in lung transplants have reached different conclusions. Sato *et al.*[37] has recently reported that chronically rejected lung grafts have evidence of lymphoid neogenesis, which are composed of T lymphocytes, B cells, and PNAd-expressing high endothelial venules. In a model of intrapulmonary tracheal transplantation, they further demonstrated that graft rejection was associated with the development of lymphoid neogenesis within the lung. However, Hasegawa *et al.*[38] reported that BALT was not associated with clinically significant acute rejection or chronic rejection of human lung grafts. In fact, BALT was found in patients, who did not develop chronic rejection, where it was also observed at earlier time points after transplantation. On the basisof these findings, the authors postulated that the development of BALT "suggested a more receptive graft environment" and "may be a manifestation of immunological tolerance". Our findings support this notion and, to our knowledge, provide the first experimental evidence that induction of BALT can be associated with an immune quiescent state.

BALT in accepted lung grafts contains markers that have been associated with immunoregulation. A large number of Foxp3$^+$ cells are located in the BALT, many of which are closely associated with CD11c$^+$ dendritic cells. Moreover, CD11c$^+$ dendritic cells express PD-L1, a ligand that is known to downregulate immune responses in part through expansion and maintenance of Foxp3$^+$ regulatory T cells.[39–41] Using intravital two-photon microscopy, we show that recipient T cells interact extensively with the CD11c$^+$ dendritic cells in accepted lung allografts.[18]

T cells were largely limited to dendritic cell-rich regions and, following extravasation, displayed low motility coefficients, velocities, and displacements similar to T-cell behaviors reported by Halle *et al.*[42] using *ex vivo* two-photon imaging of BALT induced by vaccinia virus infection. Reduced T-cell motility is a hallmark of antigen recognition *in vivo* in peripheral lymph nodes.[43,44] A characteristic feature of BALT is the development of PNAd-expressing high endothelial venules, which play an important role in the recruitment of T cells from the blood. Consistent with previous reports on BALT, the homeostatic chemokine CCL21 is expressed within the lymphoid aggregates in our accepted lung allografts.[15] Induction of BALT following respiratory viral infection and generation of adaptive immune responses within lungs is impaired in *plt*/*plt* mice that lack expression of CCL19 and CCL21.[45] Elucidating molecular mechanisms that contribute to the induction of BALT and its maintenance following pulmonary engraftment may lead to the development of new therapeutic strategies for lung transplant patients.

In conclusion, development of a technique for retransplantation in the mouse has allowed us to evaluate the impact of early alloimmunity on both rejection and acceptance of lung grafts. Unlike the case for hearts, responses occurring within lungs during the first 72 h after transplantation into immunosuppressed hosts suffice to protect the grafts from immunological destruction. Our findings indicate that early tolerogenic events play a critical role in determining long-term outcomes after lung transplantation and point to the importance of perioperative immunological management.

METHODS

Animals. C57BL/6 (H-2^b; B6), B6 CD45.1, CBA/Ca (H-$2K^k$), Balb/c (H-$2K^d$), and nude mice were purchased from The Jackson Laboratories (Bar Harbor, ME). B6 mice expressing enhanced yellow fluorescent protein driven by a CD11c promoter (CD11c-EYFP$^+$) were a gift from M Nussenzweig (Rockefeller University, New York, NY) and bred at our facility. Animal procedures were approved by our institutional Animal Studies Committee.

Lung transplantation and retransplantation. Left orthotopic vascularized lung transplants were performed using cuff techniques as described previously.[46,47] For left lung retransplants, dissection of the graft needs to be performed judiciously as adhesions form between the transplanted lung and the chest wall. The heart–lung block is removed and the left hilum is exposed in a Petri dish. The pulmonary artery and veins are divided proximal to the previously placed cuffs. The suture ligatures that had been placed during the initial transplant procedure to secure the recipient to their respective donor vessels are removed and subsequently the recipient vessels are dissected from the graft leaving the original cuffs in place. Next, the lung is flushed with 1 ml of ice-cold low potassium dextran glucose solution through the pulmonary artery. The heart–lung block is then stored in low potassium dextran glucose solution at 4 °C with the bronchus still attached. To avoid entry of preservation solution into the graft airway, the initial recipient bronchus is not removed from the graft until the time of implantation. Implantation of the left lung graft is performed by inserting cuffed donor pulmonary artery, pulmonary veins, and bronchus into the respective recipient structures and the cuffs are secured with 10-0 nylon suture ligatures. The graft is reperfused and ventilated immediately upon release of the ties and clamps that have been placed to occlude the recipient's structures. Mice weighing 22–25 g were used as donors and 26–30 g as recipients for both primary lung transplants and retransplants.

Heart transplantation and retransplantation. Cardiac grafts were transplanted or retransplanted into the right neck of recipient mice as described previously.[48] Briefly, the recipient's right external jugular vein and the right common carotic artery were dissected and occluded proximally with ties. A cuff (24 G angiocatheter) was placed on the right common carotid artery. The external jugular vein was ligated distally and a small opening made between two ligatures. The donor ascending aorta and pulmonary artery were anastomosed to the recipient's common carotid artery and external jugular vein, respectively. The cardiac graft was reperfused by releasing the ties on the recipient vessels. Grafts were monitored by daily palpation and considered rejected upon cessation of the heartbeat.

Treatment. Some lung and heart recipients were treated with MR1 (anti-CD40 ligand; 250 μg intraperitoneally, day 0) and CTLA4Ig (200 μg intraperitoneally, day 2) as described previously.[13] Some lung recipients received additional treatment with PC61 (anti-CD25 antibody; 1 mg intraperitoneally, days −1, 0, 1) (all antibodies were purchased from BIOExpress, West Lebanon, NH).

Histology. Portions of transplanted lungs and hearts were fixed in formaldehyde, sectioned, and stained with hematoxylin and eosin. Grading for acute cellular rejection was performed in a blinded manner by a pathologist (JHR) using the standard criteria. The grading scale for lung transplant rejection was as follows: grade A0: no cellular infiltrates; grade A1: minimal acute rejection with perivascular infiltrates comprising only one or two layers of predominantly small lymphocytes; grade A2: mild acute rejection with several layers of small and large lymphoid cells cuffing vessels and endothelialitis; grade A3: moderate acute rejection with spread of infiltrates into the interstitium of alveolar septae and spaces, as well as predominance of large lymphoid cells and intra-alveolar accumulation of macrophages and neutrophils; and grade A4: severe acute rejection characterized by vascular thrombosis with massive intra-alveolar hemorrhage and infarction resulting in diffuse alveolar damage with necrosis of alveolar epithelium.

Flow cytometry. Transplanted lungs were prepared for flow cytometric analysis as described previously.[12] Briefly, T lymphocyte infiltration into lungs was assessed by staining with fluorochrome-labeled anti-CD90.2 (clone 30-H12), anti-CD4 (clone RM4-5), anti-CD8 (clone 53-6.7), anti-CD45.1 (clone A20), anti-CD11c (clone HL3), anti-CD11b (clone M1/70), and anti-PD-L1 (clone MIH5), as well as their respective isotype controls (BD Biosciences, San Jose, CA and eBioscience, San Diego, CA). Intracellular staining was performed with anti-interferon-γ (clone XMG1.2), anti-Foxp3 (clone FJK-16), and the respective isotype control. For intracellular interferon-γ staining, cells were stimulated with 20 ng ml^{-1} phorbol myristate acetate (Sigma-Aldrich, St Louis, MO) and 1 μM ionomycin (Calbiochem, San Diego, CA) for 4 h, with monensin (2 μM; Sigma-Aldrich) being added for the last 3 h of culture.

Immunostaining. Lungs were prepared for immunohistochemical staining as described previously.[13] Primary antibodies and dilutions used were as follows: unlabeled polyclonal anti-CD3, 1:2,500 (immunohistochemistry) and 1:100 (immunofluorescence) (Abcam, Cambridge, MA), anti-CCL21, 1:200 (clone 59106; R&D Systems, Minneapolis, MN), anti-PNAd carbohydrate epitope, 1:50 (clone MECA-79; BD Biosciences), anti-CD45R/B220, 1:100 (immunohistochemistry) 1:50 (immunofluorescence) (clone RA3-6B2; BD Biosciences), biotin-conjugated anti-Foxp3, 1:100 (clone FJK-16s; eBioscience) and biotin-conjugated PD-L1, 1:100 (PD-L1; BioLegend, San Diego, CA). For immunohistochemistry, sections were incubated with biotinylated secondary antibody (ABC Elite; Vector Laboratories, Burlingame, CA), visualized with 3,3′-diaminobenzidine substrate solution and counterstained with hematoxylin. Secondary

antibodies for CD3 and CD45R/B220 immunofluorescence were anti-rabbit conjugated with fluorescein isothiocyanate at 1:200 (Jackson Immunoresearch, West Grove, PA) and anti-rat conjugated with Alexa Fluor 555 at 1:500 (Molecular Probes, Carlsbad, CA). Immunofluorescence staining for colocalization with CD11c-YFP was performed on frozen lung tissue sections. For Foxp3 colocalization, sections were fixed with Cytofix/Cytoperm (BD Biosciences) for 15 min at 4 °C, and then washed using Perm/Wash Buffer (BD Biosciences). For PD-L1 colocalization, sections were fixed with 4% paraformaldehyde in phosphate-buffered saline for 10 min at room temperature, and then washed with phosphate-buffered saline. Endogenous biotin was blocked with avidin/biotin blocking kit (Invitrogen, Carlsbad, CA). Primary antibody was incubated overnight at 4 °C and then binding was detected using streptavidin antibodies conjugated with Alexa Fluor 555 (Invitrogen/Molecular Probes). Slides were mounted with media containing 4′,6′ diamidino-2-phenylindole (Vector Laboratories). A Leica DM 5000B microscope (Wetzlar, Germany) was used for image capture with a Retiga 2000R charge-coupled device camera (Q Imaging, Surrey, BC, Canada) interfaced with the QCapture Pro software (Q Imaging). No detectable staining was observed for isotype-matched or species-specific control antibodies. Images were composed using the Photoshop and Illustrator software (Adobe Systems, San Jose, CA).

Two-photon imaging. Intravital two-photon imaging of lungs and lymph nodes, as well as two-photon microscopy of heart explants were performed 30 days after transplantation of Balb/c lungs or hearts, respectively, into MR1/CTLA4-Ig-treated B6 CD11c-EYFP$^+$ hosts as described previously.[18] We injected 10^7 CMTMR-labeled (Invitrogen) B6 CD90$^+$ T cells into the lung recipients 12 h before intravital imaging of lung grafts. The 655 nm non-targeted Q-dots (20 µl/100 µl) (Invitrogen) were injected intravenously. The tortuosity index of a vessel was calculated by dividing the distance along the full course of a representative vessel and the distance of a straight line between the end points of the same vessel. The tortuosity index is a measure of the straightness of a vessel, with lower values indicating a straighter line between vessel end points. Time-lapse imaging was performed with a custom-built two-photon microscope[49] running ImageWarp (A&B Software, New London, CT) for hardware control and image acquisition. At each time point, 21 sequential *z*-sections (2.5 µm each) were acquired to yield an imaging volume of 220×240×75 µm^3. Multi-dimensional rendering and manual cell tracking were performed with Imaris (Bitplane, Zurich, Switzerland).

Statistics. The unpaired two-tailed Student's *t*-test was used for statistical analysis.

SUPPLEMENTARY MATERIAL is linked to the online version of the paper at http://www.nature.com/mi

ACKNOWLEDGMENTS

D.K. and A.E.G. are supported by a grant sponsored by the The National Heart, Lung, and Blood Institute (1R01HL094601).

DISCLOSURE

The authors declared no conflict of interest.

REFERENCES

1. Kreisel, D. *et al.* Short- and long-term outcomes of 1000 adult lung transplant recipients at a single center. *J. Thorac. Cardiovasc. Surg.* **141,** 215–222 (2011).
2. Khalifah, A.P. *et al.* Minimal acute rejection after lung transplantation: a risk for bronchiolitis obliterans syndrome. *Am. J. Transplant.* **5,** 2022–2030 (2005).
3. Prop, J., Tazelaar, H.D. & Billingham, M.E. Rejection of combined heart–lung transplants in rats. Function and pathology. *Am. J. Pathol.* **127,** 97–105 (1987).
4. McGregor, C.G. *et al.* Combined heart–lung transplantation for end-stage Eisenmenger's syndrome. *J. Thorac. Cardiovasc. Surg.* **91,** 443–450 (1986).
5. Gelman, A.E. *et al.* Cutting edge: acute lung allograft rejection is independent of secondary lymphoid organs. *J. Immunol.* **182,** 3969–3973 (2009).
6. Lakkis, F.G., Arakelov, A., Konieczny, B.T. & Inoue, Y. Immunologic "ignorance" of vascularized organ transplants in the absence of secondary lymphoid tissue. *Nat. Med.* **6,** 686–688 (2000).
7. Lechler, R.I. & Batchelor, J.R. Immunogenicity of retransplanted rat kidney allografts. Effect of inducing chimerism in the first recipient and quantitative studies on immunosuppression of the second recipient. *J. Exp. Med.* **156,** 1835–1841 (1982).
8. Graca, L., Cobbold, S.P. & Waldmann, H. Identification of regulatory T cells in tolerated allografts. *J. Exp. Med.* **195,** 1641–1646 (2002).
9. Marui, T. *et al.* Histologic damage of lung allografts according to magnitude of acute rejection in the re-isotransplant model. *J. Heart Lung Transplant.* **27,** 642–648 (2008).
10. Tullius, S.G. *et al.* Contribution of early acute rejection episodes to chronic rejection in a rat kidney retransplantation model. *Kidney Int.* **53,** 465–472 (1998).
11. Izutani, H. *et al.* Evidence that graft coronary arteriosclerosis begins in the early phase after transplantation and progresses without chronic immunoreaction. Histopathological analysis using a retransplantation model. *Transplantation* **60,** 1073–1079 (1995).
12. Gelman, A.E. *et al.* CD4$^+$ T lymphocytes are not necessary for the acute rejection of vascularized mouse lung transplants. *J. Immunol.* **180,** 4754–4762 (2008).
13. Okazaki, M. *et al.* Maintenance of airway epithelium in acutely rejected orthotopic vascularized mouse lung transplants. *Am. J. Respir. Cell Mol. Biol.* **37,** 625–630 (2007).
14. Okazaki, M. *et al.* Costimulatory blockade-mediated lung allograft acceptance is abrogated by overexpression of Bcl-2 in the recipient. *Transplant Proc.* **41,** 385–387 (2009).
15. Moyron-Quiroz, J.E. *et al.* Role of inducible bronchus associated lymphoid tissue (iBALT) in respiratory immunity. *Nat. Med.* **10,** 927–934 (2004).
16. Rangel-Moreno, J. *et al.* Inducible bronchus-associated lymphoid tissue (iBALT) in patients with pulmonary complications of rheumatoid arthritis. *J. Clin. Invest.* **116,** 3183–3194 (2006).
17. Randall, T.D. Bronchus-associated lymphoid tissue (BALT) structure and function. *Adv. Immunol.* **107,** 187–241 (2010).
18. Kreisel, D. *et al. In vivo* two-photon imaging reveals monocyte-dependent neutrophil extravasation during pulmonary inflammation. *Proc. Natl. Acad. Sci. USA* **107,** 18073–18078 (2010).
19. Lindquist, R.L. *et al.* Visualizing dendritic cell networks *in vivo*. *Nat. Immunol.* **5,** 1243–1250 (2004).
20. Gelman, A.E. *et al.* CCR2 regulates monocyte recruitment as well as CD4 T1 allorecognition after lung transplantation. *Am. J. Transplant.* **10,** 1189–1199 (2010).
21. Samy, E.T., Wheeler, K.M., Roper, R.J., Teuscher, C. & Tung, K.S. Cutting edge: autoimmune disease in day 3 thymectomized mice is actively controlled by endogenous disease-specific regulatory T cells. *J. Immunol.* **180,** 4366–4370 (2008).
22. Setiady, Y.Y., Coccia, J.A. & Park, P.U. *In vivo* depletion of CD4$^+$ FOXP3$^+$ Treg cells by the PC61 anti-CD25 monoclonal antibody is mediated by FcgammaRIII$^+$ phagocytes. *Eur. J. Immunol.* **40,** 780–786 (2010).
23. Loebbermann, J. *et al.* Regulatory T cells expressing granzyme B play a critical role in controlling lung inflammation during acute viral infection. *Mucosal Immunol.* **5,** 161–172 (2012).
24. Zhang, N. *et al.* Regulatory T cells sequentially migrate from inflamed tissues to draining lymph nodes to suppress the alloimmune response. *Immunity* **30,** 458–469 (2009).
25. Constant, S.L. *et al.* Resident lung antigen-presenting cells have the capacity to promote Th2T cell differentiation *in situ*. *J. Clin. Invest.* **110,** 1441–1448 (2002).
26. Aloisi, F. & Pujol-Borrell, R. Lymphoid neogenesis in chronic inflammatory diseases. *Nat. Rev. Immunol.* **6,** 205–217 (2006).
27. Grant, A.J. *et al.* Hepatic expression of secondary lymphoid chemokine (CCL21) promotes the development of portal-associated lymphoid tissue in chronic inflammatory liver disease. *Am. J. Pathol.* **160,** 1445–1455 (2002).

28. Barone, F. *et al.* Association of CXCL13 and CCL21 expression with the progressive organization of lymphoid-like structures in Sjogren's syndrome. *Arthritis Rheum.* **52,** 1773–1784 (2005).
29. Thaunat, O. *et al.* Lymphoid neogenesis in chronic rejection: evidence for a local humoral alloimmune response. *Proc. Natl. Acad. Sci. USA* **102,** 14723–14728 (2005).
30. Wang, J. *et al.* Donor lymphoid organs are a major site of alloreactive T-cell priming following intestinal transplantation. *Am. J. Transplant.* **6,** 2563–2571 (2006).
31. Baddoura, F.K. *et al.* Lymphoid neogenesis in murine cardiac allografts undergoing chronic rejection. *Am. J. Transplant.* **5,** 510–516 (2005).
32. Nasr, I.W. *et al.* Tertiary lymphoid tissues generate effector and memory T cells that lead to allograft rejection. *Am. J. Transplant.* **7,** 1071–1079 (2007).
33. Brown, K., Sacks, S.H. & Wong, W. Tertiary lymphoid organs in renal allografts can be associated with donor-specific tolerance rather than rejection. *Eur. J. Immunol.* **41,** 89–96 (2011).
34. Sminia, T., van der Brugge-Gamelkoorn, G.J. & Jeurissen, S.H. Structure and function of bronchus-associated lymphoid tissue (BALT). *Crit. Rev. Immunol.* **9,** 119–150 (1989).
35. Moyron-Quiroz, J.E. *et al.* Persistence and responsiveness of immunologic memory in the absence of secondary lymphoid organs. *Immunity* **25,** 643–654 (2006).
36. van der Strate, B.W. *et al.* Cigarette smoke-induced emphysema: a role for the B cell? *Am. J. Respir. Crit. Care Med.* **173,** 751–758 (2006).
37. Sato, M. *et al.* The role of intrapulmonary *de novo* lymphoid tissue in obliterative bronchiolitis after lung transplantation. *J. Immunol.* **182,** 7307–7316 (2009).
38. Hasegawa, T., Iacono, A. & Yousem, S.A. The significance of bronchus-associated lymphoid tissue in human lung transplantation: is there an association with acute and chronic rejection? *Transplantation* **67,** 381–385 (1999).
39. Francisco, L.M. *et al.* PD-L1 regulates the development, maintenance, and function of induced regulatory T cells. *J. Exp. Med.* **206,** 3015–3029 (2009).
40. Krupnick, A.S. *et al.* Murine vascular endothelium activates and induces the generation of allogeneic $CD4^+25^+Foxp3^+$ regulatory T cells. *J. Immunol.* **175,** 6265–6270 (2005).
41. Wolfle, S.J. *et al.* PD-L1 expression on tolerogenic APCs is controlled by STAT-3. *Eur. J. Immunol.* **41,** 413–424 (2011).
42. Halle, S. *et al.* Induced bronchus-associated lymphoid tissue serves as a general priming site for T cells and is maintained by dendritic cells. *J. Exp. Med.* **206,** 2593–2601 (2009).
43. Mempel, T.R., Henrickson, S.E. & Von Andrian, U.H. T-cell priming by dendritic cells in lymph nodes occurs in three distinct phases. *Nature* **427,** 154–159 (2004).
44. Miller, M.J., Safrina, O., Parker, I. & Cahalan, M.D. Imaging the single cell dynamics of $CD4^+$ T cell activation by dendritic cells in lymph nodes. *J. Exp. Med.* **200,** 847–856 (2004).
45. Rangel-Moreno, J., Moyron-Quiroz, J.E., Hartson, L., Kusser, K. & Randall, T.D. Pulmonary expression of CXC chemokine ligand 13, CC chemokine ligand 19, and CC chemokine ligand 21 is essential for local immunity to influenza. *Proc. Natl. Acad. Sci. USA* **104,** 10577–10582 (2007).
46. Okazaki, M. *et al.* A mouse model of orthotopic vascularized aerated lung transplantation. *Am. J. Transplant.* **7,** 1672–1679 (2007).
47. Krupnick, A.S. *et al.* Orthotopic mouse lung transplantation as experimental methodology to study transplant and tumor biology. *Nat. Protoc.* **4,** 86–93 (2009).
48. Tomita, Y. *et al.* Improved technique of heterotopic cervical heart transplantation in mice. *Transplantation* **64,** 1598–1601 (1997).
49. Zinselmeyer, B.H. *et al.* Chapter 16. Two-photon microscopy and multidimensional analysis of cell dynamics. *Methods Enzymol.* **461,** 349–378 (2009).